

Aqueous heavy metals removal by adsorption on amine-functionalized mesoporous silica

José Aguado, Jesús M. Arsuaga, Amaya Arencibia, M. Lindo and V. Gascón*

Department of Chemical and Environmental Technology, ESCET

Universidad Rey Juan Carlos, C/ Tulipán s/n, 28933 Móstoles, Madrid, Spain

Published on Journal of Hazardous Materials 163 (2009) 213–221

<http://dx.doi.org/10.1016/j.jhazmat.2008.06.080>

*To whom correspondence should be addressed

Phone: 34 91 488 70 85

Fax: 34 91 488 70 68

E-mail: amaya.arencibia@urjc.es

Abstract

Amino functional mesoporous silica SBA-15 materials have been prepared to develop efficient adsorbents of heavy metals in wastewater. Functionalization with amino groups has been carried out by using two independent methods, grafting and co-condensation. Three organic moieties have been selected to incorporate the active amino sites: aminopropyl ($\text{H}_2\text{N}-(\text{CH}_2)_3-$), [amino-ethylamino]-propyl ($\text{H}_2\text{N}-(\text{CH}_2)_2-\text{NH}(\text{CH}_2)_3-$) and [(2-aminoethylamino)-ethylamino]-propyl ($\text{H}_2\text{N}-(\text{CH}_2)_2-\text{NH}-(\text{CH}_2)_2-\text{NH}(\text{CH}_2)_3-$). Materials have been characterized by XRD, nitrogen sorption measurements and chemical analysis. We have found that all materials preserve the mesoscopic order and exhibit suitable textural properties and nitrogen contents to act as potential adsorbents. Metal removal from aqueous solution has been examined for Cu(II), Ni(II), Pb(II), Cd(II), and Zn(II); adsorption performances of materials prepared by the two functionalization methods have been compared. In addition, copper adsorption process has been thoroughly studied from both kinetic and equilibrium points of view for some selected materials. Aqueous Cu(II) adsorption rates show that the overall process is fast and the time evolution can be successfully reproduced with a pseudo-second order kinetic model. Whole copper adsorption isotherms have been obtained at 25°C. Significant maximum adsorption capacities have been found with excellent behavior at low concentration.

Keywords: Heavy metal removal; mesoporous silica; amine-functionalized SBA-15; adsorption, wastewater treatment

1. Introduction

Removal of heavy metals from aqueous solutions is one of the major problems on wastewater treatment because they are mostly toxic even at very low concentration. These pollutants are present in water from industrial applications, including mining, refining and production of textiles, paints and dyes. A wide variety of techniques to remove heavy metals from water is available such as ion exchange, reverse osmosis and nanofiltration, precipitation, coagulation/co-precipitation and adsorption [1-2]. This last technique is very popular due to simplicity and low cost. Although activated carbon is frequently used as general adsorbent of inorganic and organic compounds, alternative adsorbents have been developed to improve the effectiveness at very low pollutant concentration. For this aim, new hybrid organic-inorganic mesoporous ordered structures have been lately proposed as heavy metals adsorbents.

The preparation of mesostructured silicas since 1992 [3] until now has opened a wide field of applications [4]. These materials are obtained by surfactant promoted alkoxysilane autoassembly methods. Mesoporous silicas present high superficial areas and large uniform pores [3, 5-7]; moreover, the silica wall surface can be modified with organic groups to tailor their properties and achieve specific purposes [8-9]. In general, functionalization of these materials can be carried out by two independent methods [8]. The first of them is carried out by grafting the surface of the preformed silica by means of silanol groups reactions with an organoalkoxysilane compound supporting the active functional group. The second method consists in the simultaneous co-condensation within the synthesis medium of the alkoxysilane precursor of the silica mesostructure and a selected organoalkoxysilane to obtain the functionalized material after one step.

Among the main uses of mesoporous silicas, it is prominent the design of selective heavy metal adsorbents for environmental clean up and many reports can be found in literature since the seminal reports [10-11].

Most of the reported works about this topic have been concerned to the functionalization with propylthiol and other thio-groups in order to remove mercury from water [10-18]. However, other heavy metals are more efficiently adsorbed on mesostructured silica modified with organic chains containing one or more amino groups [19-26]. The amine derivatives have been developed by incorporating the monoamino, diamino and triamino ligands into various families of mesoporous ordered silicas by the two independent methods mentioned above, grafting [19-20,23-24] and co-condensation [21-22, 25-28]. In addition, multi-amine functionalized materials have been also studied due to their implication in anion removal by copper-loaded amine-silica [29-32], CO₂ capture [33-34], immobilization of biological molecules [35], and basic catalysis of fine chemistry reactions [36].

Among the mesoporous silica materials, SBA-15, prepared by using poly(alkylene oxide) triblock copolymer as structure directing agent, has one of the largest pore size found for siliceous mesostructured materials [7]. Therefore, SBA-15 could be the ideal support for designing general purpose adsorbents. In particular, this work reports the study of the properties of some amine-functionalized SBA-15 silicas as heavy metal adsorbents. We have obtained SBA-15 materials functionalized with organic moieties that contain one, two or three amino functional groups. The two known synthesis routes, co-condensation and grafting, have been used to prepare the materials. In the last case, calcination and extraction methods of template removal have been compared in order to optimize the post-functionalization with amino groups and further use as heavy metal adsorbents. Our aim is to check the ability of the synthesized

materials to act as adsorbents of the following aqueous metals: copper, nickel, zinc, cadmium and lead. The last part of this research has been focused on copper in order to study the metal adsorption process in detail, analyzing both kinetic and equilibrium features.

2. Materials and Methods

2.1 Chemicals

Surfactant Pluronic P123, triblock poly(ethylene oxide)-poly(propylene oxide)-poly(ethylene oxide), (PEO₂₀PPO₇₀PEO₂₀), was used as structure directing agent. Tetraethoxysilane [TEOS; (CH₃CH₂O)₄Si] was employed as silica precursor. The organoalkoxysilanes selected for the functionalization process were aminopropyltrimethoxysilane [(H₂N-(CH₂)₃-Si(OCH₃)₃], [amino-ethylamino]-propyltrimethoxysilane [(H₂N-(CH₂)₂-NH-(CH₂)₃-Si(OCH₃)₃] and [(2-aminoethylamino)ethylamino]propyltrimethoxysilane [(H₂N-(CH₂)₂-NH-(CH₂)₂-NH-(CH₂)₃-Si(OCH₃)₃] (Table 1). These reagents were purchased from Aldrich and used without further purification. Sources of metals for sorption experiments were copper nitrate, cadmium nitrate, lead nitrate, zinc nitrate and nickel nitrate of synthesis grade that were supplied from Scharlau.

2.2 Adsorbents synthesis

2.2.1 Synthesis of amine-functionalized silica SBA-15 by grafting

Prior to the functionalization with organic chains, pure silica SBA-15 was synthesized by using Pluronic 123 triblock-copolymer according to the bibliography [7]. 4 g of Pluronic 123 were dissolved at room temperature in 125 mL of HCl 1.9 M. TEOS was added to this solution and the synthesis was carried out by stirring at 40 °C for 20 hours. Then, aging was performed at 100 °C for 24 hours. Solid product was recovered by filtration and the template removed by using two different procedures: calcination at

550°C for 5 hours (C) and extraction by ethanol refluxing (roughly 140 mL per gram of silica) during 24 hours (E). Further hydration of calcined silica surface was carried out by stirring 1 g of material C within boiling water for 4 hours (C-H).

To graft the silica surface, 1.1 g of so-obtained materials were dispersed in toluene and 4.1 mmol of organoalkoxysilane precursor were added; the mixture was refluxed for 24 hours. Solid materials were vacuum filtered and then cleaned by Soxhlet extraction in toluene. Amine-grafted silica materials were labeled G-SBA-15-N, G-SBA-15-NN, and G-SBA-15-NNN corresponding to organic chains containing one, two and three amino functional groups. Since the propylamine group was used to graft every SBA-15 prepared material (C, E and C-H), the resulting adsorbents were named as G-SBA-15-N-C, G-SBA-15-N-E, and G-SBA-15-N-C-H. However, grafting functionalization with organic chains containing two and three amino groups was solely carried out with SBA-15 purified by extraction; thus, these materials were referred to as G-SBA-15-NN-E and G-SBA-15-NNN-E.

2.2.2 *Synthesis of amine-functionalized silica SBA-15 by co-condensation*

Amine-functionalized mesoporous SBA-15 silicas obtained by co-condensation were synthesized following the procedure previously reported to incorporate other functional groups into mesostructured silica [17-18, 37]. 4 g of Pluronic P123 were dissolved at room temperature in 125 mL of HCl 1.9 M. After heating to 40°C, 37 mmol of TEOS were added to the solution that was stirred for 45 minutes before adding 4.1 mmol of the corresponding organosilane precursor (N, NN or NNN) to obtain an organosilane / TEOS molar ratio of 0.1 in the synthesis medium. The reactant mixture was stirred for 20 hours and finally aged for 24 hours at 100°C. Silica products were recovered by filtration and then dried. The template was extracted with ethanol (140 mL per gram of solid) under reflux for 24 hours and solid was filtered and dried at 100°C

for 2 hours. We denoted these materials as C-SBA-15-N, C-SBA-15-NN, and C-SBA-15-NNN.

2.3 Characterization of synthesized amine-functionalized silica SBA-15

Mesoscopic order was investigated by Low-angle X-Ray diffraction (XRD). Patterns of the samples were obtained on a powder PW3040/00 X'Pert MPD/MRD diffractometer using the $K\alpha$ Cu line. N_2 adsorption-desorption isotherms at 77 K were measured by using a Micromeritics Tristar 3000 sorptometer to determine textural properties. Surface area was calculated by using the B.E.T equation and the pore size distribution was obtained from the adsorption branch by means of the B.J.H. model with cylindrical geometry of the pores; pore volume was taken at $P/P_0 = 0.97$. Quantitative determination of the amino functional group content was measured by elemental microanalysis on a CHNOS model Vario EL III of Elementar Analyses System GMHB.

2.4 Heavy metal adsorption experiments

In order to test the metal removal ability of the synthesized materials a set of adsorption experiments was carried out by stirring 50 mg of functionalized silica in 45 mL of a single metal solution at 25°C. The aqueous systems selected were Cu(II), Pb(II), Cd(II), Zn(II) and Ni(II). Initial concentration for these experiments was 100 mg L⁻¹ and the metal salts used were nitrates in all cases. Adsorbent-solution mixtures were stirred for 24 hours and, then, filtered with a syringe filter of 0.22 μ m to collect the final solutions. Metal concentration, both in the initial and final solutions, was determined by inductively coupled plasma atomic emission spectroscopy (ICP-AES). Measurements were performed in a Varian Vista AX spectrometer after calibration with stock solutions in the range of concentration of 0-10 mg L⁻¹. The emission lines used were according to the standard EPA method for analysis of these metals [38]. Adsorbed heavy metal

amount was determined by difference between initial and final metal concentrations in the solution.

2.5 Copper adsorption experiments

The copper adsorption process in aqueous solution was studied in detail for some selected synthesized materials. The effect of contact time between solution and adsorbent along with the influence of initial Cu(II) concentration were investigated to analyze the adsorption kinetics and determine the equilibrium time. In addition, full copper adsorption isotherms were obtained from multiple equilibrium experiments.

All Cu(II) adsorption essays were conducted by the same procedure mentioned in section 2.4, but 25 mg of adsorbent mass was used in each run instead. Kinetic experiments were carried out by stopping agitation at different times selected from 5 min to 24 h. To obtain the complete isotherm, many independent runs were carried out by varying the initial metal concentration from 5 to 300 mg L⁻¹.

3. Results and discussion

3.1 Structural, textural and chemical properties of amine-functionalized SBA-15 adsorbents

As mentioned above, amine-functionalized SBA-15 materials have been prepared by grafting and co-condensation. In this section we present the results of the characterization by small angle X-Ray Diffraction (XRD), nitrogen adsorption-desorption measurements and chemical analysis of the amine-functionalized SBA-15 samples.

3.1.1 Amine-functionalized SBA-15 obtained by grafting

In this synthesis method, previous to the functionalization with amino-propyltrimethoxysilane, different template removal procedures have been investigated:

calcination (C), extraction (E) and calcination-hydration (C-H), the last intended to enhance the number of silanol groups available for the subsequent silylation reaction with the organosilane precursor [10]. XRD patterns of monoamine-grafted samples G-SBA-15-N-C, G-SBA-15-N-E and G-SBA-15-N-C-H are plotted in Figure 1; also shown is calcined pure silica SBA-15. All diffractograms exhibit the characteristic peak corresponding to the pore family (1 0 0) denoting their mesoscopic order. However, while diffractograms corresponding to pure SBA-15 and G-SBA-15-N-C clearly present the two higher order peaks of plane families (1 1 0) and (2 0 0), figure shows that the functionalization with amino groups of materials obtained from calcination-hydration and extraction procedures reduces the mesoscopic order because the intensity of secondary peaks is lower.

Figure 2 shows the adsorption-desorption isotherms of N₂ at 77 K and the corresponding pore size distributions calculated by the B.J.H. method for these amine-grafted SBA-15 materials. Textural properties obtained from the experimental isotherms are collected in Table 2. Characteristic mesoporous type IV IUPAC isotherms have been found for all materials. Adsorbed nitrogen volume decreases in the order G-SBA-15-N-E > G-SBA-15-N-C > G-SBA-15-N-C-H, because calcination produces contraction of the mesoporous structure and the posterior surface hydration leads to a smaller N₂ adsorption capacity. Pore size distributions are relatively narrow and the mean pore diameter diminishes in the order cited above (Table 2). Likewise, the highest surface area and pore volume are found for the adsorbent prepared by extraction, followed by the calcined amine-material.

Nitrogen content of the monoamine-grafted samples is shown in Table 2. As it can be seen, G-SBA-15-N-E and G-SBA-15-N-C-H contain rather similar amounts of organic group (3.1 and 2.8 mmol g⁻¹, respectively) which are significantly higher than

the corresponding to the G-SBA-15-N-C material (1.9 mmol g^{-1}). This is an expected behavior, because calcination removes a great quantity of surface silanol groups and hence, there are few organic groups incorporated to the material. However, the posterior hydration step increases the number of silanol groups available to reaction with aminopropyltrimethoxysilane and a larger amount of organic groups incorporates to the material.

Functionalization with organic chains that contain more than one amino functional group in their structure has been exclusively carried out with SBA-15 silica obtained by extraction, because this surfactant removal procedure allows incorporating higher amounts of organic chain to the silica structure. Low angle XRD diffractograms of G-SBA-15-NN-E and G-SBA-15-NNN-E samples corresponding to the materials grafted with NN and NNN are shown in Figure 3 and compared with G-SBA-15-N-E. The presence of (1 0 0) diffraction peaks as well as the weak (1 1 0) and (2 0 0) reflections indicate that all samples preserve the mesoscopic order after functionalization process.

Figure 4 shows the experimental N_2 adsorption-desorption isotherms, with their B.J.H. pore size distributions, for G-SBA-15-N-E, G-SBA-15-NN-E, and G-SBA-15-NNN-E materials; Table 2 records the corresponding textural properties. N_2 adsorption isotherm of G-SBA-15-NN-E amine-silica is clearly type IV according to IUPAC classification, but the flat isotherm of material grafted with diethylentriamine (NNN) indicates a significant reduction of porosity. Pore size distribution of G-SBA-15-NN-E is slightly narrower than that of G-SBA-15-N-E and is centered at a lower value of pore diameter. Although surface area, pore diameter and pore volume corresponding to the material prepared with ethylenediamine (NN) are smaller than found for G-SBA-15-N-E, these values are still suitable to act as good adsorbent.

Significant differences have been found for the organic chain content of materials grafted with the three different organosilane compounds. As it can be seen in Table 2, that includes the nitrogen and the organic chain contents, the molar amount of ethylenediamine and diethylenetriamine that is incorporated to the G-SBA-15-NN-E and G-SBA-15-NNN-E materials, respectively, is clearly lesser than the amount of aminopropyl anchored to the G-SBA-15-N-E sample.

3.1.2 Amine-functionalized SBA-15 adsorbents obtained by co-condensation

Direct synthesis of amine-SBA-15 materials by co-condensation was carried out to incorporate the aminopropyl, diethylenaminopropyl and ethylenetriaminopropyl groups into the mesoporous structure. Figure 5 shows the XRD diffractograms of C-SBA-15-N, C-SBA-15-NN and C-SBA-15-NNN. In all cases, it can be observed the intense peak corresponding to the (1 0 0) pore family and the two additional weak reflections assigned to the family planes (1 1 0) and (2 0 0) which are indicative of high hexagonal mesoscopic order.

The nitrogen adsorption-desorption isotherms of samples obtained by co-condensation along with their pore size distributions are plotted in Figure 6 where calcined SBA-15 pure silica is also shown for comparison. As seen, no significant differences are observed in the isotherms of the three amine-functionalized SBA-15 materials. All of them are type IV according to the IUPAC classification and exhibit a similar decrease of adsorption capacity compared with pure silica due to the organic functionalization. Pore size distributions also are very alike and show a mean pore diameter of *ca.* 8.2 nm as read in Table 2. Values of surface area and pore volume likewise are lower than the values of the pure silica; this behavior indicates that textural

properties for the resulting amine mesoporous materials are rather independent of the specific amino organosilane group incorporated to the silica material.

Nitrogen and organic groups contents of the amine-materials functionalized by co-condensation are recorded in Table 2. The amount of organic chain incorporated to the materials C-SBA-15-N and C-SBA-15-NN is very similar, nearly 1 mmol g^{-1} ; however, a significant lower content is found for C-SBA-15-NNN. This behavior has been previously also observed for other authors and indicates that the introduction of diethylentriamine in the mesoporous structure is a difficult task [25, 34].

3.2 Heavy metal removal evaluation

A first group of experiments has been carried out to test the ability of synthesized materials to act as heavy metal adsorbents, pure silica SBA-15 included. Aqueous solutions of metal concentration 100 mg L^{-1} have been stirred in presence of 50 mg of each amine-functionalized adsorbent at 25°C and the essays have been repeated for copper nitrate, lead nitrate, cadmium nitrate, zinc nitrate and nickel nitrate. Pure SBA-15 experiments yield null adsorption at this detection level, so metal loading of the modified SBA-15 samples should exclusively attribute to the presence of active amino groups anchored to the silica walls.

However, no detectable adsorption has been observed from the experiments performed with the amine-SBA-15 materials functionalized by co-condensation in spite of their significant nitrogen content and good structural and textural properties. Negligible adsorption values denote that amino groups incorporated to the material are not accessible to the metallic species. As it has been already pointed by other authors, since SBA-15 synthesis is conducted in strong acidic medium, the protonated amines can interact with both the surfactant and the silicate species [27]. These interactions lead

to the incorporation of the organic chains inside the silica walls and, hence, to the absence of available sites for heavy metal adsorption in contrast with other materials amine-functionalized by co-condensation under neutral or basic conditions [25-26].

Conversely, materials functionalized by grafting with monoamine, diamine and triamine organic chains (G-SBA-15-N-C, G-SBA-15-N-C-H, G-SBA-15-N-E, G-SBA-15-NN-E, and G-SBA-15-NNN-E) exhibit remarkable metal withdrawal capacities as shown in Figure 7, where removal percentages of the tested metals are displayed. This graph suggests that there are three different sorption performances depending on the specific metal. Aqueous Pb(II) adsorption percentage clearly is the biggest for all materials here studied with measured values around 100%. Cd(II) removal is intermediate between lead behavior and the percentages corresponding to the group of Ni(II), Cu(II) and Zn(II) which adsorption is rather similar. Nevertheless, it should be realized that an inattentive glance to Figure 7 may lead to misunderstanding conclusions. Considering that initial mass concentration is the same for all experiments, namely 100 mg L^{-1} , molar concentration depends on the atomic weight of each metal; therefore, lead solutions are almost four times more dilute in molar scale than nickel solutions. Consequently, the nitrogen anchoring points to metal species number ratio decreases in the sequence $\text{Pb} \gg \text{Cd} \gg \text{Zn} \geq \text{Cu} \geq \text{Ni}$, the same diminution order found for adsorption percentage. So, the three distinctive behaviors mentioned above should be analyzed in an individual way. Moreover, to determine both the maximum adsorption capacity of each adsorbent and the efficiency at low concentration, which are two crucial parameters to design an adsorption process for heavy metal removal, it is necessary to obtain global kinetic information and determine the whole adsorption equilibrium isotherm for every metal.

In this work, copper has been selected to carry out the first complete study of the adsorption process on amine-grafted SBA-15 materials as representative of the behavior observed for the Ni(II)/Cu(II)/Zn(II) group.

3.3 Specific study of aqueous copper adsorption

3.3.1. Copper adsorption kinetics

A detailed study of the adsorption rate was carried out for G-SBA-15-NN-E, a material chosen as representative of the whole behavior. For this purpose, a collection of copper solutions with the same initial concentrations was stirred at 200 r.p.m. in the presence of adsorbent constant amounts. Stirring was stopped at different selected times and solutions were filtered and analyzed. This experimental routine was repeated for three initial aqueous Cu(II) concentrations: 5, 113, and 263 mg L⁻¹. Rough experimental data are recorded in Figure 8 that shows the final copper concentration against contact time. As seen, the significant metal concentration decrease quickly occurs in the early stages of the process. Although solution concentration remains changeless after 120 min, an agitation time of 180 min has been selected for the subsequent adsorption equilibrium experiments, a value in accordance with previously reported for other functionalized SBA-15 adsorbents [39]. Similar results have been obtained in this work for the equilibrium time ascribed to the other amine-functionalized adsorbents.

Adsorption rate has been analyzed by using two common semi-empirical kinetic models which are based on adsorption equilibrium capacity: the pseudo-first order and pseudo-second order equations, proposed by Lagergren [40] and Ho and McKay [41], respectively.

Pseudo-first order equation relates the adsorption rate to the metal adsorbed amount at time t as:

$$\frac{dq_t}{dt} = k_1 (q_e - q_t) \quad (1)$$

where q_e and q_t are, respectively, the adsorbed amounts of metal at equilibrium and time t , expressed as mmol g^{-1} ; k_1 is the pseudo-first order kinetic constant, expressed as min^{-1} . Equation integration and rearrangement yield the lineal form:

$$\ln (q_e - q_t) = \ln q_e - k_1 t \quad (2)$$

Pseudo-second-order equation may be written in the form:

$$\frac{dq_t}{dt} = k_2 (q_e - q_t)^2 \quad (3)$$

where k_2 is the pseudo-second order kinetic constant, expressed as $\text{g mmol}^{-1} \text{min}^{-1}$. The differential equation is usually integrated and transformed in its linear form:

$$\frac{t}{q_t} = \frac{1}{k_2 q_e^2} + \frac{t}{q_e} \quad (4)$$

Linear arrangements, eq. 2 and 4, are commonly used to check the validity of these models and to obtain the model parameters when the corresponding linear plot is adequate. Figure 9 shows some examples of both linear plots. It is clear from Figure 9a that pseudo-first order model is not suitable to describe the kinetic profile because of the apparent lack of linear behavior. Conversely, rates of aqueous Cu(II) adsorption over diamine-grafted SBA-15 material are accurately described by the pseudo-second-order equation, as shown in Figure 9b where experimental t/q_t and t data are provided along with linear correlations for the three sets of experiments. Table 3 summarizes the calculated parameters q_e^{calc} and k_2 for each initial copper concentrations, C_0 ; regression coefficients r obtained from linear fits indicate a regular good correlation. Experimental results of adsorbed copper amount at equilibrium obtained after stirring 24 hours, q_e^{exp} , are also included in Table 3. As seen, these C_0 dependent values are in very good agreement with the calculated from the kinetic model. Pseudo-second order constants

diminish from 3.58 to 0.23 g mmol⁻¹ min⁻¹ when initial copper concentration rises from 5 to 263 mg L⁻¹. A similar evolution has been previously observed for other functionalized SBA-15 materials prepared for mercury adsorption [39].

3.3.2. Copper adsorption isotherms

Full adsorption isotherms have been obtained at 25°C for the amine-grafted materials G-SBA-15-N-C, G-SBA-15-N-E, G-SBA-15-N-C-H and G-SBA-15-NN-E. Isotherms have been constructed as an aggregate of many separate experimental runs. Each essay has been carried out by stirring 25 mg of adsorbent with 45 mL of aqueous solutions which initial copper concentrations range from 5 to 300 mg L⁻¹. Figure 10a displays the isotherms where the amount of copper adsorbed at equilibrium, q_e (milimol per gram of adsorbent), is plotted as a function of the resulting aqueous Cu(II) concentration, C_e , (mg L⁻¹). All the isotherms show a sharp initial slope so indicating that materials act as high efficacy adsorbents at low metal concentration; in addition, when aqueous Cu(II) concentration increases a saturation constant value is reached. This behavior corresponds to Langmuir isotherm, or L2-type according to the Giles classification [42], which mathematical expression is:

$$q_e = \frac{Q_0 b C_e}{1 + b C_e} \quad (5)$$

where Q_0 and b are the characteristic Langmuir parameters. Q_0 is the maximum adsorption capacity that it is the amount of metal to form a complete monolayer and b is a constant related to the intensity of adsorption. To obtain the model parameters the linearized Langmuir equation is mostly used:

$$\frac{C_e}{q_e} = \frac{1}{Q_0 b} + \frac{C_e}{Q_0} \quad (6)$$

Linear Langmuir plots are shown in Figure 10b where it can be seen that successful fits to experimental data are thoroughly achieved. Table 4 displays the calculated parameters Q_0 corresponding to the Langmuir model and the nitrogen and organic chain content for the four selected adsorbents; experimental maximum adsorption capacities Q_0^{exp} , obtained as the mean value of q_e in flat region of the isotherm, are also shown. The accordance between estimated and experimental Q_0 values is excellent.

Figure 10a and Table 4 evidence that copper maximum adsorption capacity Q_0 of SBA-15 functionalized with propylamine is significantly smaller than nitrogen content, an expected behavior due to the multiple coordination needed to form stable Cu(II)-amine complexes (*i.e.* one copper atom requires several amino positions). In addition, copper loading for calcinated G-SBA-15-N-C is lower than Q_0 corresponding to G-SBA-15-N-E and G-SBA-15-N-C-H materials, as presumed because materials prepared after extraction and calcination-hydration include a higher content of amino groups (around 3 against 1.9 mmol g⁻¹). However, adsorption capacities of monoamine-grafted SBA-15 materials prepared in this work are generally lower than values previously reported for other mesoporous silicas [19, 24]. So, Lam *et al.* have found that nitrogen to maximum copper adsorbed molar ratio for NH₂-MCM-41 ranges between 2.7 and 4 [24], whereas N to Cu(II) molar ratio of materials of this work varies from 7 to 9. The observed difference is attributed to the larger pore size of SBA-15 silica which induces a wide monoamino groups spreading that reduces the chance for multiamine-copper binding. Perhaps, this is why the pore contracted G-SBA-15-N-C-H exhibits a higher Q_0 than G-SBA-15-N-E material in spite of its lower nitrogen content.

Copper adsorption on G-SBA-15-NN-E silica prepared with two amino groups per organic chain is significantly enhanced with respect to materials functionalized with

aminopropyl. A maximum adsorption capacity around 0.83 mmol g^{-1} has been determined, a large value in accordance with bibliographic data [21, 25]. It should be mentioned that Q_0 increase for the diamine G-SBA-15-NN-E compared to monoamine materials notably surpasses the nitrogen content rise. So, the presence of two amine positions in the same organic chain reinforces the copper adsorption capacity through a cooperative effect due to nitrogen proximity reasons.

4. Conclusions

Mesoporous materials SBA-15 amine-functionalized with organic chains containing one, two and three amino functional groups have been synthesized by grafting and co-condensation to achieve heavy metal adsorbents from aqueous solution. Materials prepared by co-condensation show negligible metal adsorption capacity because amino active sites are not accessible to metallic species despite their suitable nitrogen content and textural properties. Conversely, amine-grafted materials, that exhibit adequate mesoscopic order and high amino groups content (up to $6.0 \text{ mmol N g}^{-1}$), adsorb significant amounts of aqueous Cu(II), Cd(II), Pb(II), Ni(II) and Zn(II). Copper adsorption process has been investigated in detail as representative of the global behavior assigned to Ni(II), Cu(II), and Zn(II). Kinetics study reveals that copper adsorption rate is fast and can be satisfactorily modeled by a pseudo-second order equation. Full isotherms of Cu(II) adsorption have been assembled for four amine-functionalized SBA-15 materials. All adsorbents are very efficient at low metal concentration and substantial amounts of Cu(II) can be removed from water. The presence of two amino positions in the same organic chain enhances the copper adsorption capacity.

Acknowledgements

Authors thank to the regional government of Madrid that has financed this work through the research project “REMTAVARES” (S-0505/AMB/0395) and to the “Ministerio de Educación y Ciencia” for the financial support through the projects CTM2005-01053 and “CONSOLIDER INGENIO 2010” (CSD2006-44).

References

- [1] H.F. Freeman, *Standard Handbook of Hazardous Waste Treatment and Disposal*, McGraw–Hill, New York, 1989.
- [2] N. P. Cheremisinoff, *Handbook of Water and Wastewater Treatment Technologies*. Ed. Butterworth and Heineman, 2002.
- [3] C. T. Kresge, M. E. Leonowicz, W. J. Roth, J. C. Vartuli, J. S. Beck, Ordered mesoporous molecular sieves tailored using different synthesis conditions. *Nature* 359 (1992) 710-713.
- [4] A. Taguchi, F. Schüth, Ordered mesoporous materials in catalysis, *Micropor. Mesopor. Mater.* 77 (2005) 1-45.
- [5] P. T. Tanev, T. J. Pinnavaia, A neutral templating route to mesoporous molecular sieves, *Science* 267 (1995) 865-867.
- [6] S. A. Bagshaw, E. Prouzet, T. J. Pinnavaia, Templating of mesoporous molecular sieves by nonionic polyethylene oxide surfactants, *Science* 269 (1995) 1242-1245.
- [7] D. Zhao, J. Feng, Q. Huo, N. Melosh, G. H. Fredrickson, B. F. Chmelka, G. D. Stucky, Triblock copolymers synthesis of mesoporous silica with periodic 50 to 300 angstrom pores, *Science* 279 (1998) 548-561.
- [8] A. Stein, B. J. Melde, R. C. Schrodin, Hybrid inorganic-organic mesoporous silicates-nanoscope reactors coming of age, *Adv. Mater.* 12 (2000) 1403-1445.
- [9] A. Vinu, K. Z. Hossain, K. Ariga, Recent advances in functionalization of mesoporous silica, *J. Nanosci. Nanotechnol.* 5 (3) (2005) 347-371.

- [10] X. Feng, G. E. Fryxell, L. Q. Wang, A. Y. Kim, J. Liu, K. M. Kemmer, Functionalized monolayers on ordered mesoporous supports, *Science* 276 (1997) 923-925.
- [11] L. Mercier, T. J. Pinnavaia, Access in mesoporous materials: advantages of uniform pore structure in the design of a heavy metal ion adsorbent for environmental remediation, *Adv. Mater.* 9 (1997) 500-507.
- [12] J. Brown, R. Richer, L. Mercier, One-step synthesis of high capacity mesoporous Hg²⁺ adsorbents by non-ionic surfactant assembly, *Micropor. Mesopor. Mater.* 37 (2000) 41-48.
- [13] R. I. Nooney, M. Kalyanaraman, G. Kennedy, E. J. Maggin, Heavy metal remediation using functionalized mesoporous silicas with controlled macrostructure, *Langmuir* 17 (2001) 528-533.
- [14] V. Antochshuck, O. Olkhovyk, M. Jaroniec, In-S. Park, R. Ryoo, Benzoylthiourea-modified mesoporous silica for mercury(II) removal, *Langmuir* 19 (2003) 3031-3034.
- [15] O. Olkhovyk, M. Jaroniec, Ordered mesoporous silicas with 2,5-dimercapto-1,3,4-thiadiazole ligand: high capacity adsorbents for mercury ions, *Adsorption* 11 (2005) 205-214.
- [16] S. J. L. Billinge, E. J. McKimmy, M. Shatnawi, H. Kim, V. Petkov, D. Wermeille, T. J. Pinnavaia, Mercury binding sites in thiol-mesostructured silica, *J. Am. Chem. Soc.* 127 (2005) 8492-8498.
- [17] J. Aguado, J. M. Arsuaga, A. Arencibia, Adsorption of aqueous mercury(II) on propylthiol-functionalized mesoporous silica obtained by co-condensation, *Ind. Eng. Chem. Res.* 44 (2005) 3665-3671.

- [18] J. Aguado, J. M. Arsuaga, A. Arencibia, Influence of synthesis conditions on mercury adsorption capacity of propylthiol functionalized SBA-15 obtained by co-condensation, *Micropor. Mesopor. Mater.* 109 (2008) 513-524.
- [19] A. M. Liu, K. Hidajat, S. Kawi, D. Y. Zhao, A new class of hybrid mesoporous materials with functionalized organic monolayers for selective adsorption of heavy metal ions, *Chem. Commun.* (2000) 1145-1946.
- [20] H. Lee, J. Yi, Removal of copper using functionalized mesoporous silica in aqueous solution, *Sep. Sci. Technol.* 36 (2001) 2433-2444.
- [21] B. Lee, Y. Kim, H. Lee, J. Yi, Synthesis of functionalized porous silicas via templating method as heavy metal ion adsorbents: the introduction of surface hydrophilicity onto the surface of adsorbents, *Micropor. Mesopor. Mater.* 77 (2001) 50-59.
- [22] M. C. Burleigh, S. Dai, C. E. Barnes, Z. L. Xue, Enhanced ionic recognition by functionalized mesoporous sol-gel: Synthesis and metal ion selectivity of diaminoethane derivative, *Sep. Sci. Technol.* 36 (15) (2001) 3395-3409.
- [23] K. F. Lam, K. L. Yeung, G. McKay, An investigation of gold adsorption from a binary mixture with selective mesoporous silica adsorbents, *J. Phys. Chem. B* 110 (2006) 2187-2194.
- [24] K.F. Lam, K. L. Yeung, G. McKay, A rational approach in the design of selective mesoporous adsorbents, *Langmuir* 22 (2006) 9632-9641.
- [25] L. Bois, A. Bonhomme, A. Ribes, B. Pais, G. Raffin, F. Tessier, Functionalized silica for heavy metal ions adsorption, *Colloids and Surfaces A: Physicochem. Eng. Aspects* 221 (2003) 221-230.

- [26] T. Yokoi, H. Yoshitake, T. Yamada, Y. Kubota, T. Tatsumi. Amino-functionalized mesoporous silica synthesized by an anionic surfactant templating route, *J. Mater. Chem.* 16 (2006) 1125-1135.
- [27] A. S. M. Chong, X. S. Zhao, Functionalization of SBA-15 with APTES and characterization of functionalized materials, *J. Phys. Chem. B* 107 (2003) 12650-12657.
- [28] X. Wang, S. Lin, K. K. Lin, J. C. C. Chan, S. Cheng, Preparation of ordered large pore SBA-15 silica functionalized with aminopropyl groups through one-pot synthesis, *Chem. Commun.* (2004) 2762-2763.
- [29] H. Yoshitake, T. Yokoi, T. Tatsumi, Adsorption behavior of arsenate at transition metal cations captured by amino-functionalized mesoporous silica, *Chem. Mater.* 15 (2003) 1713-1721.
- [30] H. Yoshitake, T. Yokoi, T. Tatsumi, Adsorption of chromate and arsenate by amino-functionalized MCM-41 and SBA-1, *Chem. Mater.* 14 (2002) 4603-4610.
- [31] S. D. Kelly, K. M. Kemmer, G. E. Fryxell, J. Liu, S. V. Mattigod, K. F. Ferris, X-Ray Absorption fine-structure spectroscopy study of the interactions between contaminant tetrahedral anions and self-assembled monolayer on mesoporous supports, *J. Phys. Chem. B.* 105 (2001) 6337-6346.
- [32] G. E. Fryxell, J. Liu, T. A. Hauser, Z. Nie, K. F. Ferris, S. Mattigod, M. Gong, R. Hallen, Design and synthesis of selective mesoporous anion traps, *Chem. Mater.* 11 (1999) 2148-2154.
- [33] G. P. Knowles, J. V. Graham, S. W. Delaney, A. L. Chaffe, Aminopropyl-functionalized mesoporous silicas as CO₂ adsorbents, *Fuel Process. Technol.* 86 (2005) 1435-1448.

- [34] G. P. Knowles, J. V. Delaney, A. L. Chaffe, Diethylenetriamine[propyl(silyl)]-Functionalized (DT) mesoporous silicas as CO₂ adsorbents, *Ind. Eng. Chem. Res.* 45 (2006) 2626-2633.
- [35] P. H. Pandya, R. V. Jasra, B. L. Newalkar, P. N. Bhatt, Studies on the activity and stability of immobilized α -amylase in ordered mesoporous silicas, *Micropor. Mesopor. Mater.* 7 (2004) 67-77.
- [36] X. Wang, J. C. C. Chan, Y-H Tseng, S. Cheng, Synthesis, characterization and catalytic activity of ordered SBA-15 materials containing high loading of diamine functional groups, *Micropor. Mesopor. Mater.* 95 (2006) 57-65.
- [37] D. Margolese, J. A. Melero, S. C. Christiansen, B. F. Chmelka, G. D. Stucky, Direct syntheses of ordered SBA-15 mesoporous silica containing sulfonic acid groups, *Chem. Mat.* 12 (2000) 2448-2459.
- [38] EPA Method 200.7. Trace elements in water, solids and biosolids by inductively coupled plasma atomic emission spectrometry, EPA-821-R-01-010. January (2001).
- [39] J. M. Arsuaga, J. Aguado, A. Arencibia, Kinetics of mercury adsorption on thiol functionalized SBA-15 mesoporous silica, Submitted to *Ind. Eng. Chem. Res.*
- [40] S. Lagergren, About the theory of the so-called adsorption of soluble substances. *Kungliga Svenska Vetenskapsakademius. Handlingar* 24 (1898) 1-39.
- [41] Y. S. Ho, G. McKay, Kinetic model for Pb sorption on peat, *Adsorpt. Sci. Technol.* 16 (1998) 243-255.
- [42] C. H. Giles, D. Smith, A. Huitson, A general treatment and classification of the solute adsorption isotherm, *J. Coll. Interf. Science* 47 (1974) 755-765.

Table captions

Table 1. Organic chains used to functionalize the silica surface.

Table 2. Textural and structural properties of amine SBA-15 synthesized materials by grafting (G) and co-condensation (C).

Table 3. Effect of Cu(II) initial concentration on adsorption kinetics. Parameters obtained from the linearized pseudo-second order model.

Table 4. Nitrogen and organic chain contents and maximum copper adsorption, Q_0 , from experimental and Langmuir-modeled adsorption isotherms.

Figure captions

Figure 1. Low-angle XRD patterns of propylamine-functionalized SBA-15 materials by grafting.

Figure 2. Nitrogen adsorption-desorption isotherms at 77 K and pore size distributions of propylamine-functionalized SBA-15 materials by grafting.

Figure 3. Low-angle X ray diffractograms of SBA-15 materials grafted with N, NN and NNN groups.

Figure 4. Nitrogen adsorption-desorption isotherms at 77 K and pore size distributions of SBA-15 materials grafted with N, NN and NNN groups.

Figure 5. Low-angle XRD diffractograms of SBA-15 materials functionalized with N, NN and NNN groups by co-condensation.

Figure 6. Nitrogen adsorption-desorption isotherms at 77 K and pore size distributions of SBA-15 materials functionalized with N, NN and NNN groups by co-condensation.

Figure 7. Removal percentage of Cu(II), Ni(II), Zn(II), Cd(II) and Pb(II) by amine-grafted adsorbents G-SBA-15. 50 mg of adsorbent and 45 mL of 100 mg L⁻¹ aqueous metal solutions were thoroughly used.

Figure 8. Temporal evolution of Cu(II) concentration after adsorption on G-SBA-15-NN-E for three initial copper concentrations.

Figure 9. Modeling of Cu(II) adsorption kinetics on G-SBA-15-NN for three initial concentrations. Linear plots of a) pseudo-first order model; b) pseudo-second order model.

Figure 10. a) Experimental copper adsorption isotherms at 25°C for monoamine and ethylenediamine SBA-15 materials functionalized by grafting. b) Linearized Langmuir plots for the same systems.

Table 1.

Organic radical	Chemical formula	Symbol
Aminopropyl (AP)	$-\text{CH}_2\text{CH}_2\text{CH}_2\text{NH}_2$	-N
Ethylendiaminopropyl (ED)	$-\text{CH}_2\text{CH}_2\text{CH}_2\text{NHCH}_2\text{CH}_2\text{NH}_2$	-NN
Diethylentriaminopropyl (DT)	$-\text{CH}_2\text{CH}_2\text{CH}_2\text{NHCH}_2\text{CH}_2\text{NHCH}_2\text{CH}_2\text{NH}_2$	-NNN

Table 2.

Materials	D_p BJH (nm)	S_{BET} ($\text{m}^2 \text{g}^{-1}$)	V_p ($\text{cm}^3 \text{g}^{-1}$)	N (mmol g^{-1})	Org. chain (mmol g^{-1})
SBA-15 silica	9.1	790	1.44	-	-
G-SBA-15-N-C	7.2	345	0.58	1.9	1.9
G-SBA-15-N-C-H	6.4	178	0.28	2.8	2.8
G-SBA-15-N-E	9.0	565	1.02	3.1	3.1
G-SBA-15-NN-E	7.3	246	0.46	4.0	2.0
G-SBA-15-NNN-E	-	48	0.09	6.0	2.0
C-SBA-15-N	8.2	572	0.87	0.9	0.95
C-SBA-15-NN	8.3	508	0.78	1.9	0.95
C-SBA-15-NNN	8.1	477	0.74	1.8	0.6

Table 3.

C_0 (mg L ⁻¹)	q_e (mmol g ⁻¹)		k_2 (g mmol ⁻¹ min ⁻¹)	r
	q_e^{calc}	q_e^{exp}		
5	0.146	0.14	3.58	0.99995
113	0.656	0.65	0.61	0.99997
263	0.846	0.82	0.23	0.996

Table 4.

Material	N (mmol g ⁻¹)	Org. Chain (mmol g ⁻¹)	Q_0^{exp} (mmol Cu g ⁻¹)	Langmuir isotherm	
				Q_0 (mmol Cu g ⁻¹)	r
G-SBA-15-NN-E	4.0	2.0	0.82	0.83	0.997
G-SBA-15-N-C-H	2.8	2.8	0.39	0.39	0.9991
G-SBA-15-N-E	3.1	3.1	0.35	0.35	0.9993
G-SBA-15-N-C	1.9	1.9	0.25	0.24	0.9998

Figure 1.

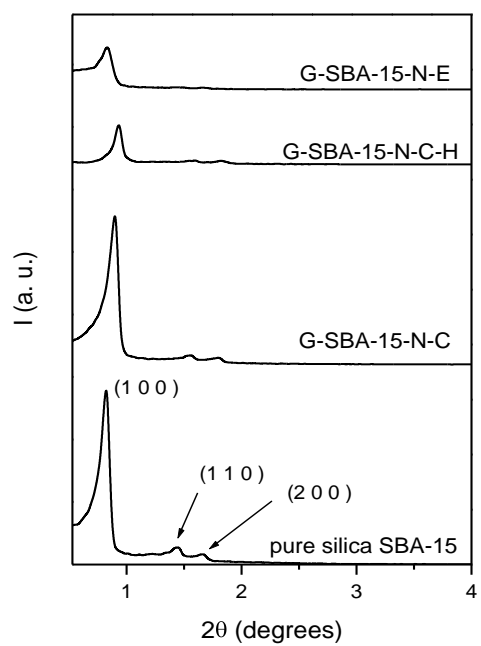


Figure 2.

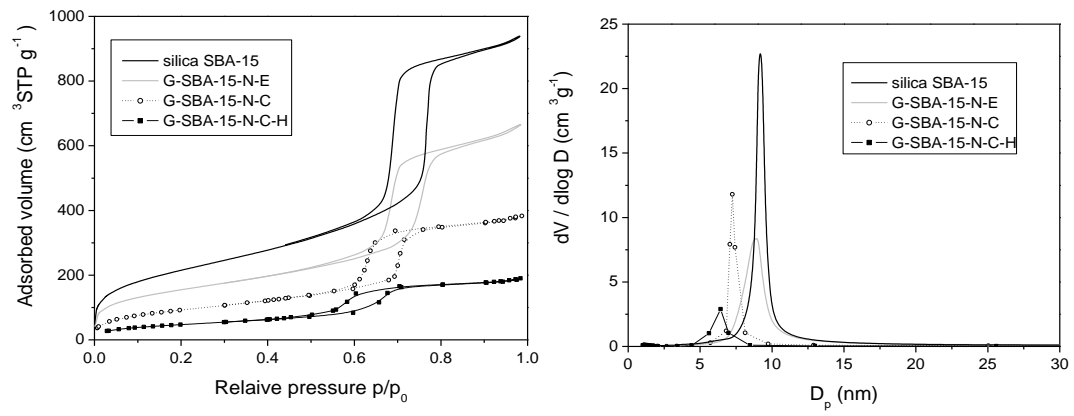


Figure 3.

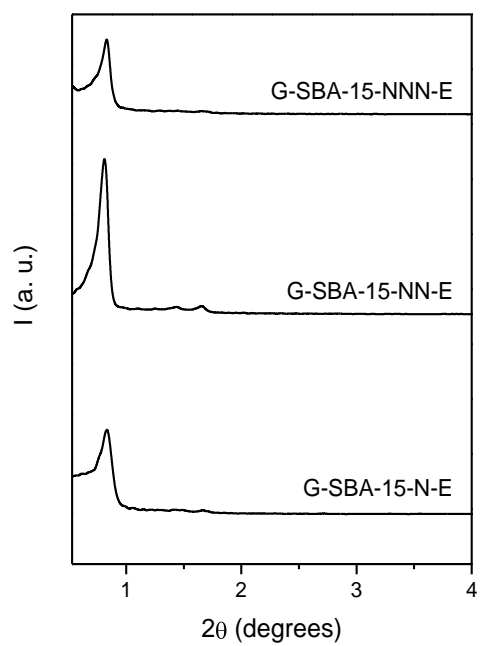


Figure 4.

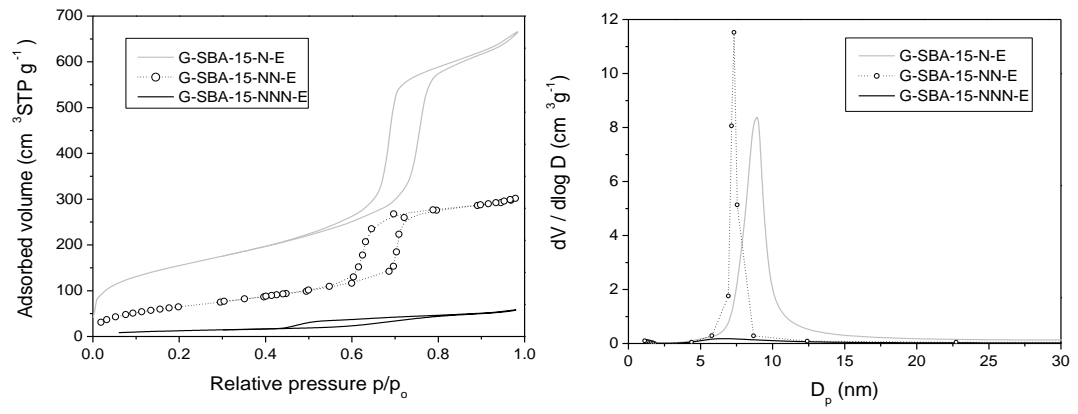


Figure 5.

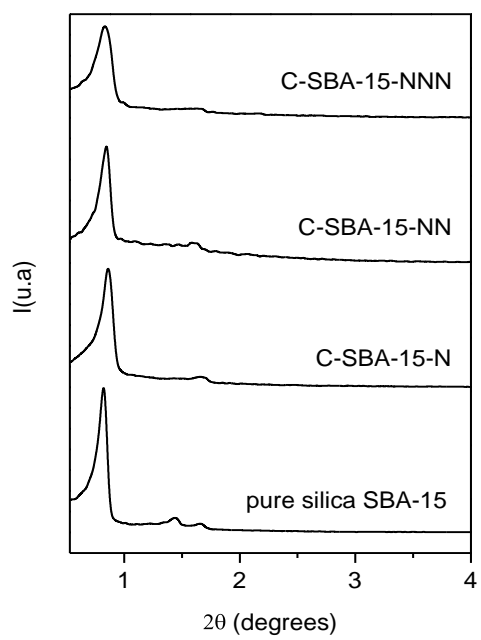


Figure 6.

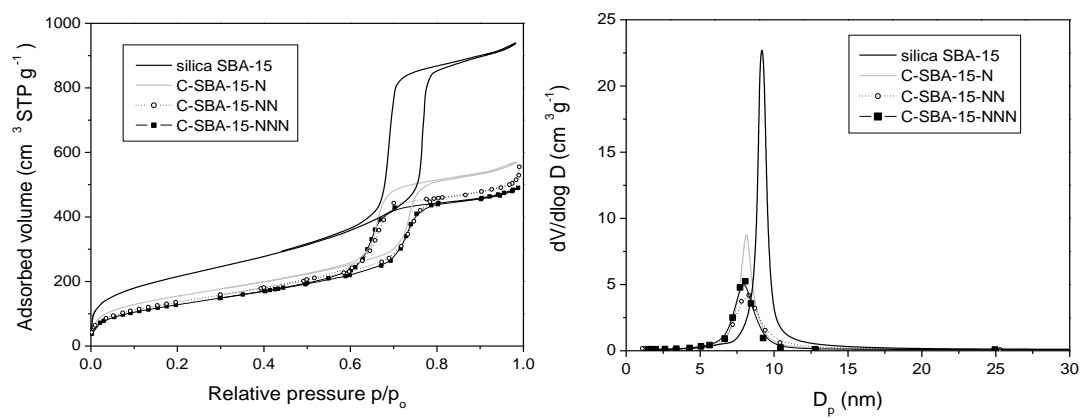


Figure 7.

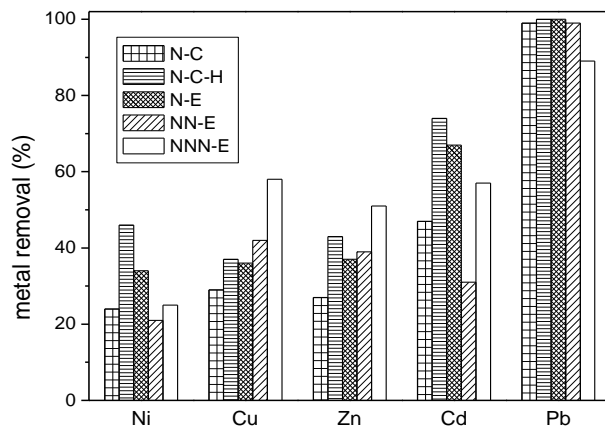


Figure 8.

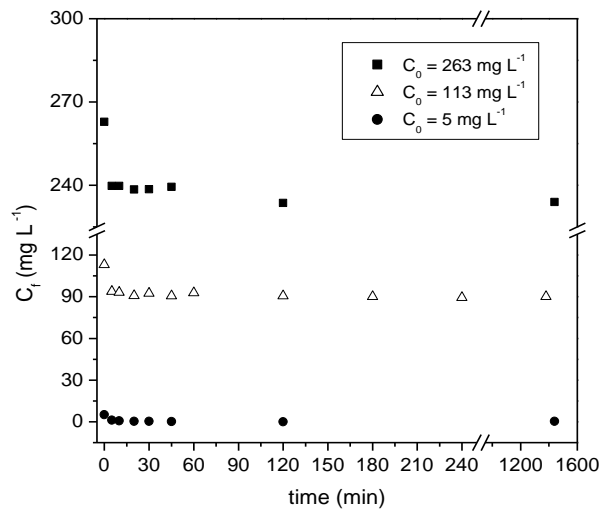


Figure 9.

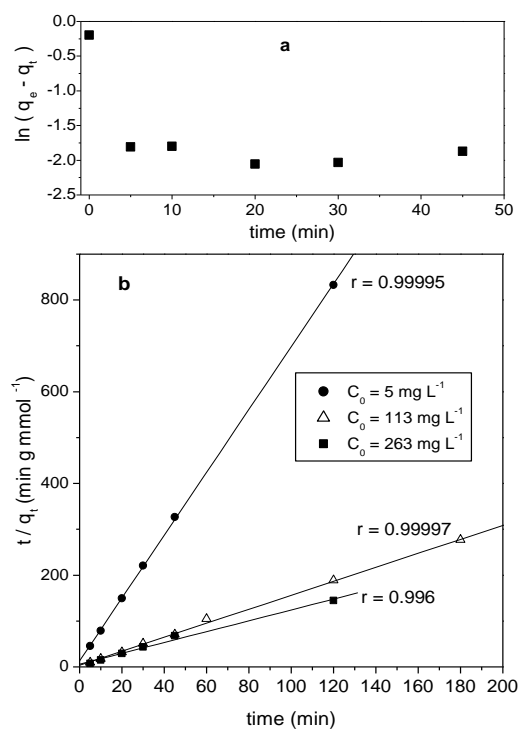


Figure 10.

